

# Dielectric Properties of the Mixed Aurivillius Phases $M^{II}Bi_8Ti_7O_{27}$ ( $M^{II} = Ca, Sr, Ba$ and $Pb$ )

R. Maalal, M. Manier & J. P. Mercurio\*

Laboratoire de Matériaux Céramiques et Traitements de Surface, URA CNRS no. 320, Faculté des Sciences, Université de Limoges, 123, Avenue Albert-Thomas, 87060 Limoges Cedex, France

(Received March 1995; revised version received 18 May 1995; accepted 19 May 1995)

## Abstract

*Ceramic materials have been prepared by natural sintering and hot-forging  $M^{II}Bi_8Ti_7O_{27}$  ( $M^{II} = Ca, Sr, Ba$  and  $Pb$ ) powders synthesized using a molten salt technique. The materials are ferroelectric at room temperature and show strong dielectric anisotropy in connection with the crystal structure. In each case, a double anomaly of the dielectric permittivity was found as a function of temperature. The temperatures at which it occurs are dependent on  $M^{II}$ . The origin of this phenomenon is assumed to be closely related to a sequence of phase transitions like those already observed in other mixed Aurivillius phases.*

## 1 Introduction

The so-called Aurivillius phases are a family of layer bismuth compounds generally formulated as  $Bi_2A_{m-1}B_mO_{3m+3}$ . Their crystal structure can be regarded as a regular intergrowth of  $(Bi_2O_2)^{2+}$  layers and  $(A_{m-1}B_mO_{3m+1})^{2-}$  perovskite-type slabs.<sup>1,2</sup> In these compounds, A is a mono-, di- or trivalent element allowing dodecahedral coordination, B is a transition element suited to octahedral coordination and  $m$  an integer ( $1 \leq m \leq 8$ ) which represents the number of perovskite-like slabs intercalated between the  $(Bi_2O_2)^{2+}$  layers. As they generally show ferroelectric behaviour, a number of them, e.g.  $Bi_2PbNb_2O_9$  ( $m = 2$ ),  $Bi_4Ti_3O_{12}$  ( $m = 3$ ),  $BaBi_4Ti_4O_{15}$  ( $m = 4$ ), have been thoroughly investigated from the point of view of both structural and electric properties.<sup>3–7</sup> The frequent occurrence of disordered intergrowths — corresponding to different values of  $m$  — suggested that ordered intergrowths would be obtained in suitable systems and under appropriate thermal treatment. In fact, various ordered intergrowths have been

recently prepared as macroscopic pure phase.<sup>8,9</sup> They always correspond to a regular intergrowth of one half the unit cell of a  $m$  member structure and one half the unit cell of a  $m + 1$  member structure, so that they have the general formula  $Bi_4A_{2m-1}B_{2m+1}O_{6m+9}$ , e.g.  $Bi_5TiNbWO_{15}$  (intergrowth  $1 + 2$ ),  $Bi_7Ti_4NbO_{21}$  (intergrowth  $2 + 3$ ) and  $M^{II}Bi_8Ti_7O_{27}$  (intergrowth  $3 + 4$ ). Several papers have been devoted to the dielectric properties of  $Bi_7Ti_4NbO_{21}$ : the main characteristic of this ferroelectric phase is the occurrence of a double anomaly of the dielectric permittivity as a function of temperature.<sup>9,10</sup> An interpretation of this phenomenon was recently given from single crystal structure investigations.<sup>11</sup> On the contrary, there is only few literature dealing with dielectric properties of phases with  $1 + 2$  or  $3 + 4$  intergrowths.

The aim of this paper is to present the results of the investigation of the dielectric properties of  $M^{II}Bi_8Ti_7O_{27}$  ( $M^{II} = Ca, Sr, Ba$  and  $Pb$ ) as a function of temperature and frequency and to discuss their evolution within the Aurivillius family.

## 2 Experimental

Polycrystalline powders were prepared by molten salt synthesis. Stoichiometric mixtures of reagent grade  $M^{II}CO_3$ ,  $Bi_2O_3$  and  $TiO_2$  were thoroughly mixed with excess NaCl–KCl eutectic and ground in agate mill for 2 h. The mixtures, placed in closed platinum crucibles were heated up to 650°C for 1 h to ensure homogenization and then soaked at 800–900°C (depending on the composition) for 1 h. After cooling, the salt was eliminated by washing with hot water until the last washing water does not react with silver nitrate and the powders finally dried at 100°C.

Ceramic samples were obtained by natural sintering of uniaxially pressed pellets at 1050–1120°C for 1–3 h in air. High oriented materials were elaborated by a hot-forging technique (920–1060°C, 4–12 MPa, 1–3 h) described elsewhere.<sup>10</sup>

\*To whom correspondence should be addressed.

The morphology of powders and the microstructure of hot-forged ceramics were observed with a Philips XL30 scanning electron microscope. X-ray diffraction patterns were obtained with a Siemens D5000 powder diffractometer (CuK $\alpha$ ) and the cell parameters refined by a least-squares method. Dielectric measurements were made between room temperature and 1000°C by impedance spectrometry using a HP 4194A impedance analyser. Disk-shaped samples (10 mm diameter and 1 mm thick) of naturally sintered ceramics and parallelepipedic bodies of hot-forged materials ( $1 \times 1 \times 3$  mm<sup>3</sup>) were polished and coated with platinum paste (Cerdec Pt 576402/1, 1000°C, 30 min), aged overnight at 110°C and left for at least 24 h before measurements. For hot-forged ceramics, electrodes were put on faces either parallel or perpendicular to the forging direction. D-E hysteresis loops were obtained at room temperature using a classical Sawyer–Tower device operating at 20 mHz. Piezoelectric coefficients  $d_{33}$  were determined with a Berlincourt-meter and the electromechanical coupling factors were derived from resonance–antiresonance measurements.

### 3 Results and Discussion

#### 3.1 Powders

Strongly anisotropic platelet-like powders were obtained using molten salt synthesis. As shown in Fig. 1 for calcium and lead compounds, they develop large faces with areas in the range 1–10  $\mu\text{m}^2$  and thickness less than 0.1  $\mu\text{m}$ . As expected, X-ray diffraction patterns confirmed that the direction perpendicular to the main faces correspond to the

stacking direction of the Bi<sub>2</sub>O<sub>2</sub> sheets. All the compounds are orthorhombic with lattice parameters  $a$  and  $b$  close to 0.54 nm ( $\approx \sqrt{2} a_{\text{perovskite}}$ ) and  $c$  inherently long ( $\approx 7.3$  nm) due to the number of perovskite and Bi<sub>2</sub>O<sub>2</sub> slabs involved in the unit cell. The evolutions of the lattice parameters are

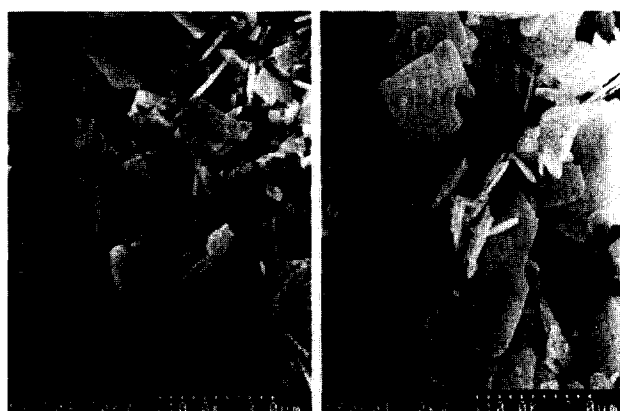


Fig. 1. SEM micrographs of CaBi<sub>8</sub>Ti<sub>7</sub>O<sub>27</sub> and PbBi<sub>8</sub>Ti<sub>7</sub>O<sub>27</sub> powders prepared by molten salt synthesis.

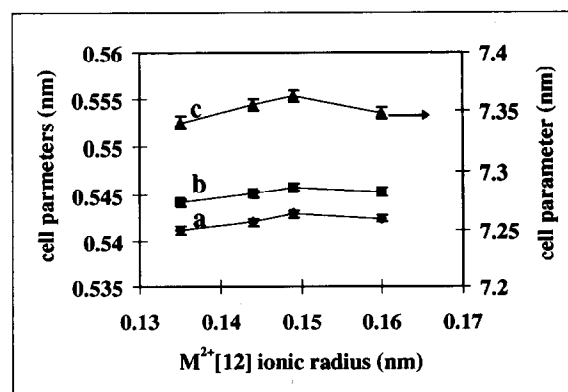


Fig. 2. Lattice parameters of  $M^{\text{II}}\text{Bi}_8\text{Ti}_7\text{O}_{27}$  as a function of  $M^{2+}$  ionic radii in coordinence.<sup>12</sup>

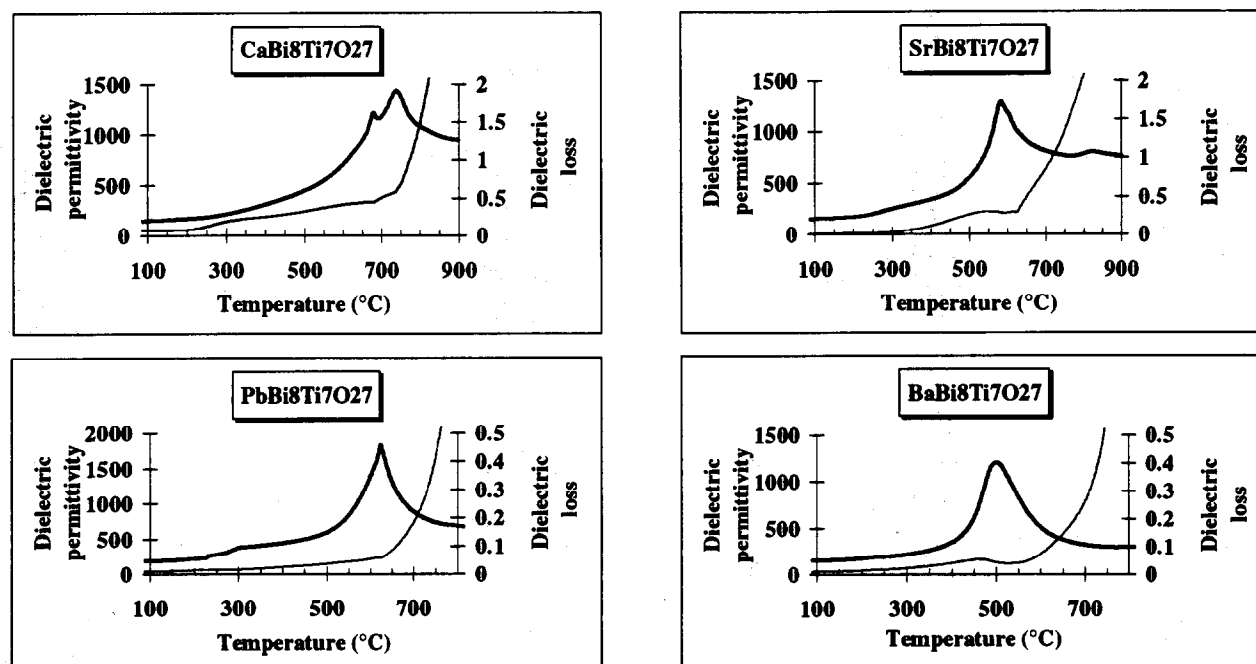


Fig. 3. Thermal variation of dielectric permittivity and loss of naturally sintered  $M^{\text{II}}\text{Bi}_8\text{Ti}_7\text{O}_{27}$  ceramics at 1 MHz.

given in Fig. 2 as a function of the ionic radii in coordinence [12] of the  $M^{2+}$  cations.<sup>12</sup> From calcium to barium, the lattice parameters roughly increase, but the behaviour of the lead compound appears to be out of the general trend. The abnormally high values obtained for this compound would be undoubtedly related to the strong polarizability of  $Pb^{2+}$  due to the  $6s^2$  lone pair which is absent in the alkaline earth compounds. Such a trend was already observed in  $M^{II}$ -containing Aurivillius phases, e.g.  $M^{II}Bi_2Nb_2O_9$ ,  $M^{II}Bi_4Ti_4O_{15}$  or  $(M^{II})_2Bi_4Ti_5O_{18}$ .<sup>3,4</sup>

### 3.2 Naturally sintered ceramics

After natural sintering in air atmosphere, ceramic materials achieved densities lying within 92–96%

of theoretical and X-ray patterns did not show any significant preferential orientation.

The thermal variations of the dielectric permittivity and dielectric loss at 1 MHz of  $M^{II}Bi_8Ti_7O_{27}$  are given in Fig. 3. For  $M^{II} = Sr, Ba$  and  $Pb$ , one dielectric anomaly is observed at 580, 480 and 610°C respectively for both  $\epsilon_r$  and  $\tan \delta$ . This behaviour was already found by Kikuchi *et al.*<sup>9</sup> On the contrary, the calcium compound is characterized by a double anomaly at 660 and 720°C, similar to that observed in the 'mixed phase'  $Bi_7Ti_4NbO_{21}$ .<sup>9,10</sup> For all compounds, the anomaly temperatures of  $\epsilon_r$  and  $\tan \delta$  are frequency independent and only a slight decrease of  $\epsilon_r$  as the frequency increases from 100 kHz to 5 MHz is observed as shown in Fig. 4.

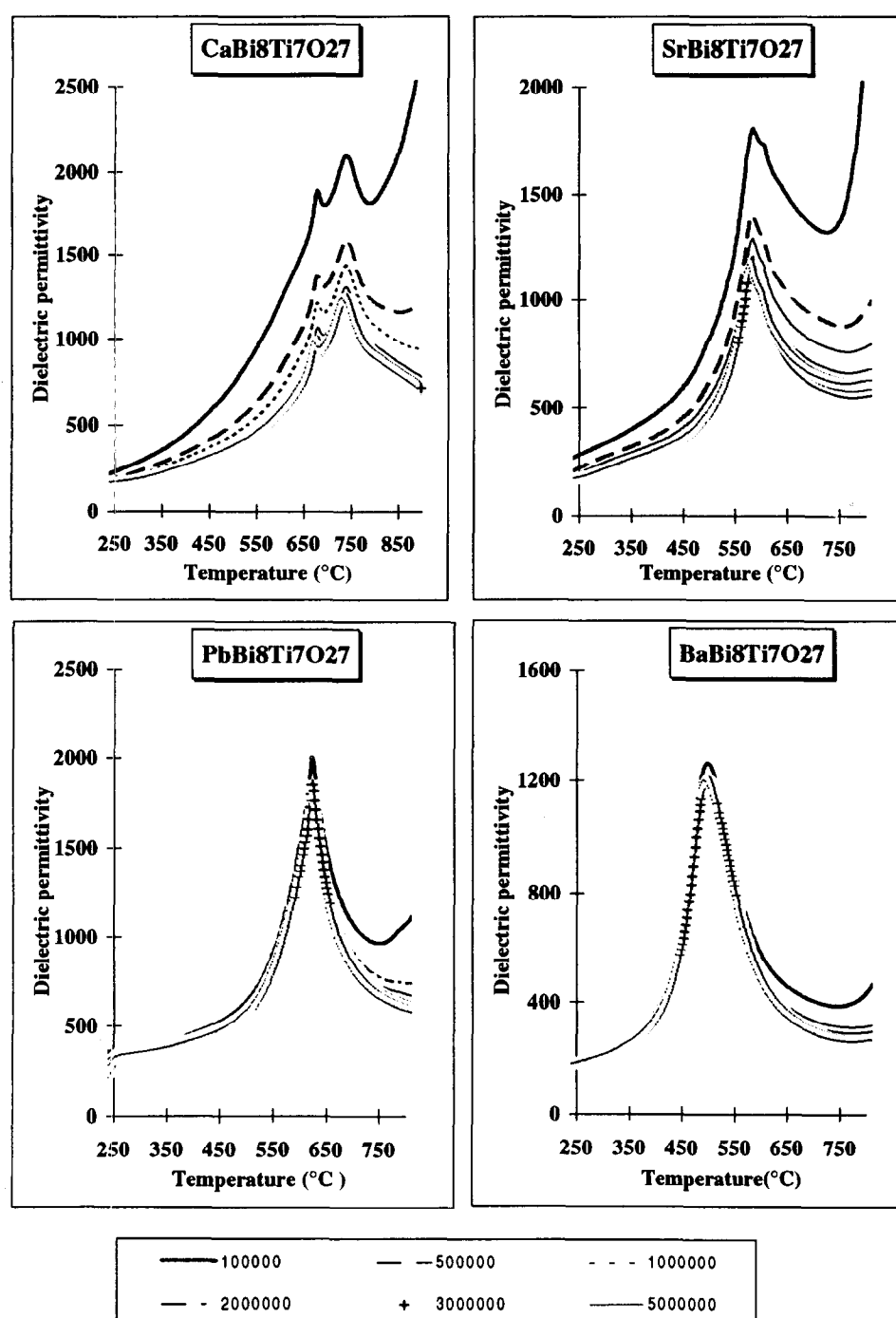


Fig. 4. Thermal variation of dielectric permittivity of naturally sintered  $M^{II}Bi_8Ti_7O_{27}$  ceramics as a function of frequency.

Polarization–electric field curves confirm the ferroelectric behaviour of these compounds at room temperature. The observed loops are not fully saturated due to experimental difficulties (Fig. 5). Nevertheless they allow determination of coercive field ( $42\text{--}58\text{ kVcm}^{-1}$ ) and remnant polarization ( $2.3\text{--}3.9\text{ }\mu\text{C cm}^{-2}$ ), (Table 1). These values are slightly lower — but of the same order of magnitude — than those obtained for  $\text{Bi}_7\text{Ti}_4\text{NbO}_{21}$ .

Table 1 also shows the piezoelectric constants  $d_{33}$  and the planar electromechanical coupling coefficients measured on samples poled at  $200^\circ\text{C}$  for 10 min in silicone oil under  $8\text{ kV mm}^{-1}$ . As for other

**Table 1.** Selected ferroelectric and piezoelectric data of  $\text{M}^{II}\text{Bi}_8\text{Ti}_7\text{O}_{27}$  naturally sintered ceramics

	Coercive field (kV/mm)	Remanent polarization ( $\mu\text{C}/\text{Cm}^2$ )	$d_{33}$ (pC/N)	$k_p$ (%)
$\text{CaBi}_8\text{Ti}_7\text{O}_{27}$	58	3.3	7.4	3.3
$\text{SrBi}_8\text{Ti}_7\text{O}_{27}$	48	3.9	8	3.2
$\text{PbBi}_8\text{Ti}_7\text{O}_{27}$	45	3.35	6.3	2.2
$\text{BaBi}_8\text{Ti}_7\text{O}_{27}$	42	2.3	7.5	2.8

Aurivillius phases, the obtained values are quite low, but are kept almost the same up to about  $450^\circ\text{C}$ .

### 3.3 Hot-forged ceramics

The hot-forging technique gave strongly oriented highly densified ceramics. Orientation factors — calculated using the Lotgering method — higher than 90% were currently obtained at  $1050^\circ\text{C}$  under 12 MPa.<sup>13</sup> The corresponding densities were 96–99% of theoretical. Figure 6 shows a SEM micrograph of the lead compound taken in a direction perpendicular to the forging axis. The strong anisotropy was confirmed by X-ray diffraction experiments performed along two perpendicular directions ( $\parallel$  and  $\perp$  to the forging axis) and compared with the powder pattern. As expected, the  $\perp$  pattern shows only (001) lines which are absent in the  $\parallel$  pattern (Fig. 7).

The thermal variations of the dielectric permittivity of hot-forged samples were measured along both  $\parallel$  and  $\perp$  directions. As previously noticed for naturally sintered materials, the temperatures of

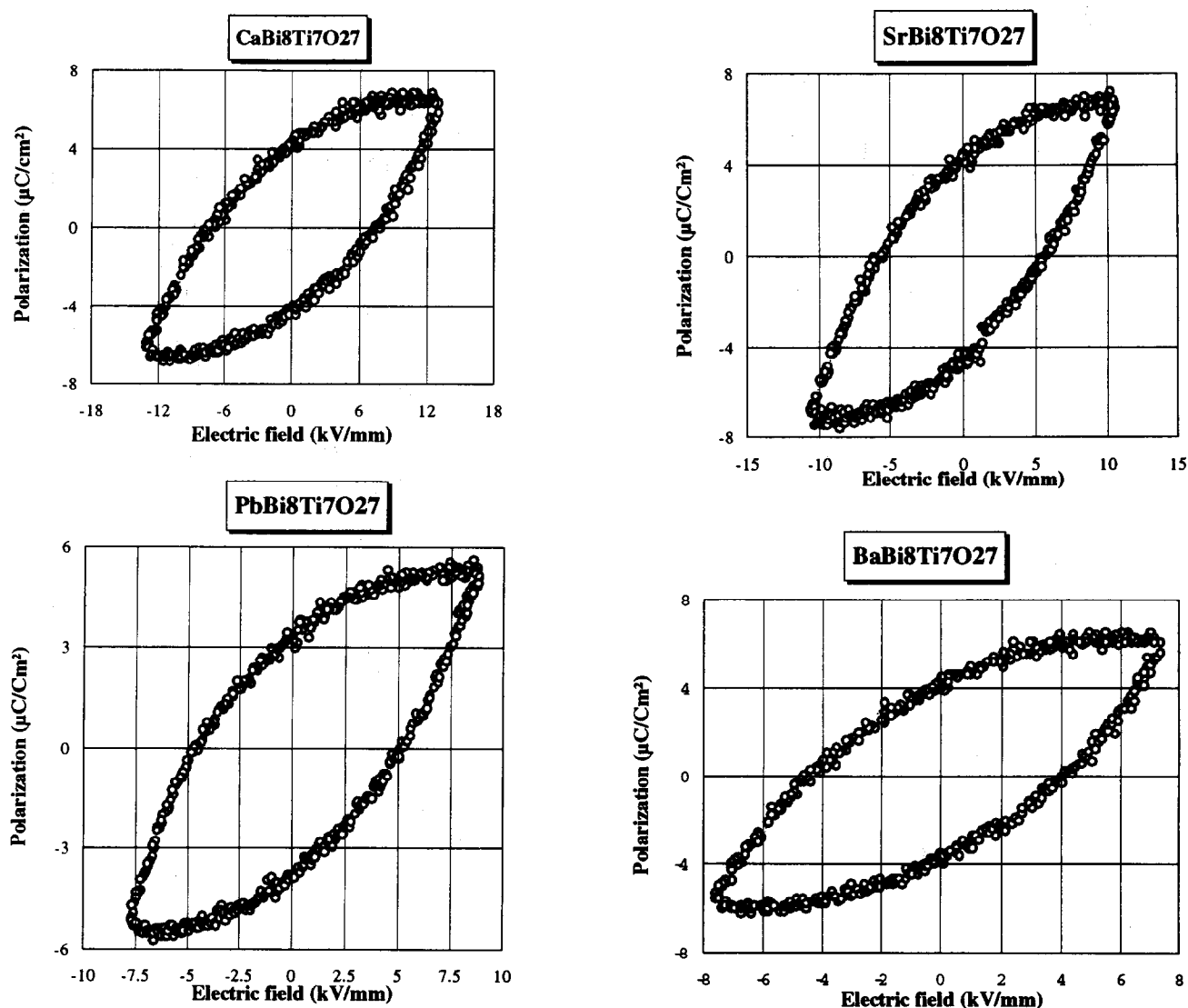


**Fig. 5.** Polarization–electric field loops of naturally sintered  $\text{M}^{II}\text{Bi}_8\text{Ti}_7\text{O}_{27}$  ceramics.



Fig. 6. SEM micrograph of hot-forged  $\text{PbBi}_8\text{Ti}_7\text{O}_{27}$  ( $\perp$  to the forging direction)

the permittivity anomalies are frequency independent. From Fig. 8, which gives the results obtained at 1 MHz, two main features can be emphasized:

- (i) in each case,  $\epsilon_{\perp}$  is higher than  $\epsilon_{\parallel}$ , the ratio being maximum at anomaly temperatures. Such a behaviour was already observed for other hot-forged materials, e.g.  $\text{M}^{\text{II}}\text{Bi}_4\text{Ti}_4\text{O}_{15}$  and  $\text{Bi}_7\text{Ti}_4\text{NbO}_{21}$ , and was attributed to the strong anisotropic microstructure of the materials.<sup>10,14</sup> As a matter of fact, the high  $\epsilon_{\perp}$  value was correlated to the direction of the polarization which lies, for most Aurivillius phases, in or close to the planes of the  $\text{Bi}_2\text{O}_2$ /perovskite sheets, i.e. perpendicular to the forging direction. In the same way, the slight maxima observed for  $\epsilon_{\parallel}$ , would indicate the presence of a small component of the polarization along the direction parallel to the forging direction (the  $c$ -axis of the unit cell).<sup>15</sup>
- (ii) in contrast with the results obtained on naturally sintered ceramics, all  $\epsilon(T)$  curves show a double anomaly more or less defined according to the  $\text{M}^{2+}$  cation (for  $\text{M} = \text{Pb}$ , there is only a small hump just before the maximum). In any case, when  $\text{M}$  is an alkaline earth element, the gap between the temperatures of the anomalies decreases when the ionic radii increase.

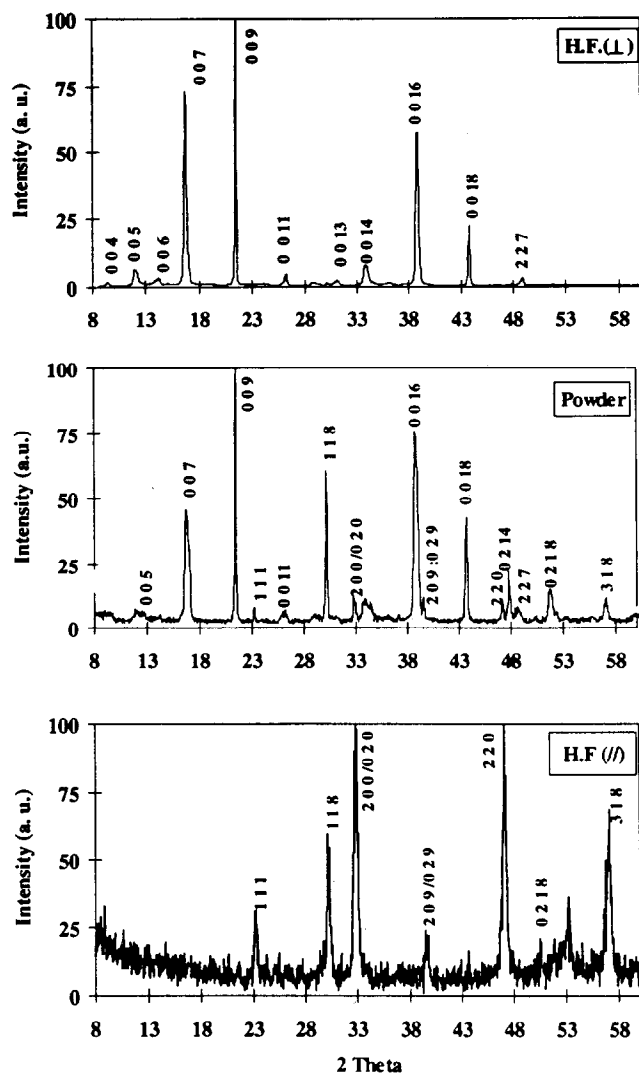


Fig. 7. X-ray diffraction patterns of hot-forged  $\text{PbBi}_8\text{Ti}_7\text{O}_{27}$  ceramics.

By reference to  $\text{Bi}_7\text{Ti}_4\text{NbO}_{21}$  (mixed 2–3 Aurivillius phase), one may suppose that the double anomaly would originate in a sequence of phase transitions of the following type: orthorhombic ferroelectric-(elastic) state I  $\rightarrow$  orthorhombic ferroelectric-(elastic) state II  $\rightarrow$  tetragonal paraelectric-(elastic) state.

The first phase transition within the orthorhombic symmetry might not occur for the lead compound because the behaviour of the lone pair  $\text{Pb}^{2+}$  cannot be strictly likened to the spherical alkaline earth cations.

#### 4 Conclusion

Dielectric experiments on naturally sintered and highly oriented hot-forged ceramics of the so-called mixed Aurivillius family  $\text{M}^{\text{II}}\text{Bi}_8\text{Ti}_7\text{O}_{27}$  have shown that all materials:

- are ferroelectric with Curie temperatures in the range 500–740°C depending on the nature of  $\text{M}^{\text{II}}$ ;

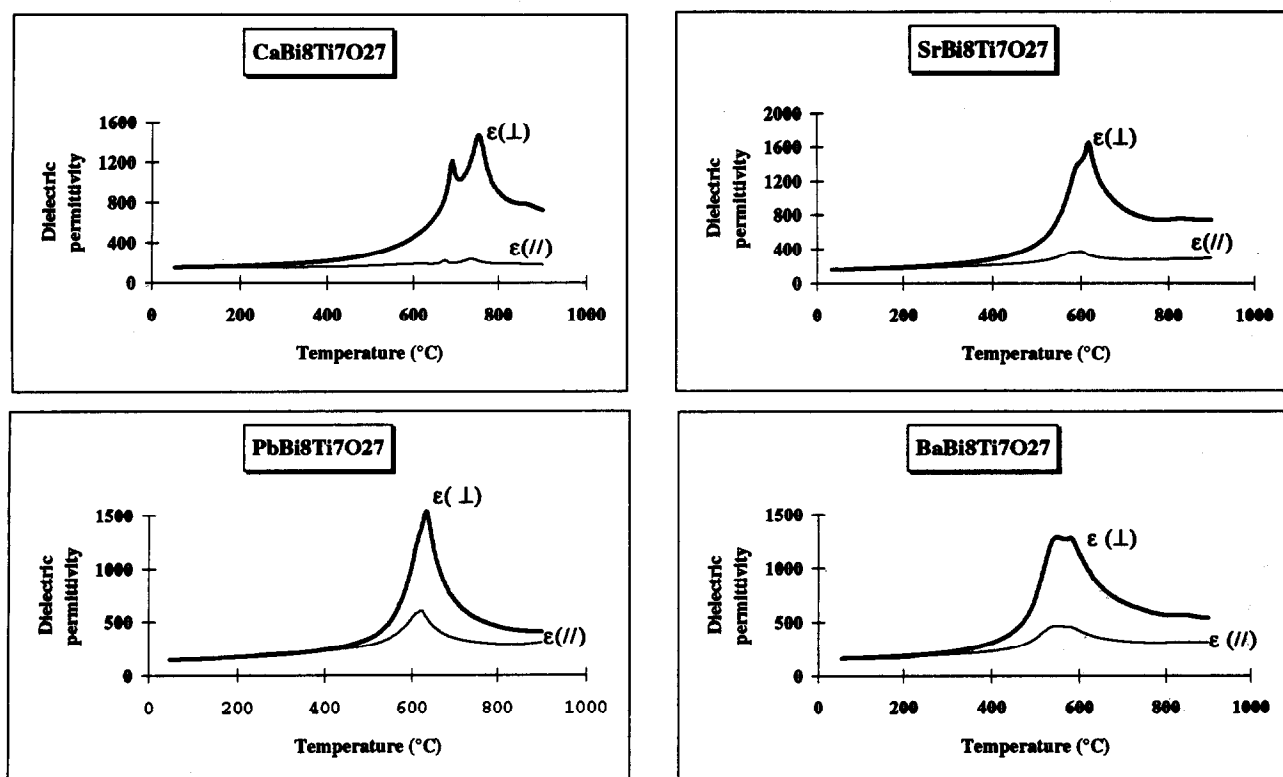


Fig. 8. Thermal variation of the dielectric permittivity of hot-forged  $M^{II}Bi_8Ti_7O_{27}$  ceramics at 1 MHz ( $\perp$  and  $\parallel$  to the forging direction).

— present a double dielectric anomaly as a function of temperature.

The overall behaviour of the ceramics is likely to that already observed in other mixed Aurivillius phases. To confirm the assumptions about the nature of the phase transitions, further investigations (crystal structure determination, dielectric and optical microscopy measurements as a function of temperature) are now in progress on  $CaBi_8Ti_7O_{27}$  single crystal.

### Acknowledgement

The authors would like to thank E. Lattard for her help in dielectric hysteresis measurements.

### References

1. Aurivillius, B., Mixed bismuth oxides with layer lattices I. The structure type of  $CaNb_2Bi_2O_9$ , *Arkiv Kemi*, **1** (1949) 463–80.
2. Aurivillius, B., Mixed bismuth oxides with layer lattices II. Structure of  $Bi_4Ti_3O_{12}$ , *Arkiv Kemi*, **1** (1949) 499–512.
3. Smolenskii, G. A., Isupov, V. A. & Agranovskaya, A. I., Seignetteoelectrics of the octahedral type with a layer structure, *Fiz. Tverdogo Tela*, **3**, (1961) 895–901.
4. Subbarao, E. C., Crystal chemistry of mixed bismuth oxides with layer-type structure, *J. Amer. Ceram. Soc.*, **45** (1962) 166–9.
5. Newnham, R. E., Wolfe, R. W. & Dorrian, J. F., Structural basis of ferroelectricity in bismuth titanate family, *Mat. Res. Bull.*, **6** (1971) 1029–39.
6. Kubel, F. & Schmid, H., X-ray room temperature structure from single crystal data, powder diffraction measurements and optical studies of the Aurivillius phase  $Bi_5(Ti_3Fe)O_{15}$ , *Ferroelectrics*, **129** (1992) 101–12.
7. Withers, R. L., Thompson, J. G. & Rae, A. D., The crystal chemistry underlying ferroelectricity in  $Bi_4Ti_3O_{12}$ ,  $Bi_3(TiNbO_9)$  and  $Bi_2WO_6$ , *J. Solid State Chem.*, **94** (1991) 404–17.
8. Horiuchi, S., Kikuchi, T. & Goto, M., Structure determination of a mixed-layer bismuth titanate  $Bi_7Ti_4NbO_{21}$  by super-high-resolution electron microscopy, *Acta Crystallogr.*, **A33** (1977) 701–5.
9. Kikuchi, T., Watanabe, A. & Uchida, K., A family of mixed-layer type bismuth compounds, *Mat. Res. Bull.*, **12** (1977) 299–304.
10. Maalal, R., Manier, M., Mercurio, J. P. & Frit, B., Grain-oriented  $Bi_7Ti_4NbO_{21}$  ceramics, *Silicates Ind.*, **5-6** (1994) 161–3.
11. Maalal, R., Propriétés diélectriques et structurales de la phase d'Aurivillius mixte  $Bi_7Ti_4NbO_{21}$ , PhD thesis, University of Limoges, France, 1994.
12. Shannon, R. D. & Prewitt, C. T., Effective ionic radii in oxides and fluorides, *Acta Crystallogr.*, **B25** (1969) 925–46.
13. Lotgering, F. K., Topotactical reactions with ferrimagnetic oxides having hexagonal crystal structures—I, *J. Inorg. Nucl. Chem.*, **9** (1959) 113–23.
14. Takenaka, T. & Sakata, K., Grain orientation and electrical properties of hot-forged bismuth titanium oxide ( $Bi_4Ti_3O_{12}$ ) ceramics, *Jpn. J. Appl. Phys.*, **19**(1) (1980) 31–9.
15. Cummins, S. E. & Cross, L. E., Electrical and optical properties of ferroelectric  $Bi_4Ti_3O_{12}$  single crystal, *J. Appl. Phys. Lett.*, **39**(5) (1968) 2268–74.